Nonlinear Phenomena in Complex Systems, vol. **16**, no. 2 (2013), pp. 146 - 161

Non-equilibrium Stochastic Dynamics of Open Ion Channels

R. Tindjong and I. Kaufman
Department of Physics, Lancaster University, Lancaster LA1 4YB, UK

D. G. Luchinsky*
Mission Critical Technologies Inc., 2041 Rosecrans Ave. Suite 225 El Segundo, CA 90245, USA

P. V. E. McClintock†
Department of Physics, Lancaster University, Lancaster LA1 4YB, United Kingdom

I. Khovanov
School of Engineering, University of Warwick, Coventry CV4 7AL, UK

R. S. Eisenberg
Department of Molecular Biophysics and Physiology,
Rush Medical College, 1750 West Harrison, Chicago, IL 60612, USA
(Received 15 February, 2013)

We present and discuss a modified version of reaction rate theory (RRT) to describe the passage of a positive ion through a biological ion channel. It takes explicit account of the non-equilibrium nature of the permeation process. Unlike traditional RRT, it allows for the non-constant transition rates that arise naturally in an archetypal model of an ion channel. In particular, we allow for the fact that the average escape time of an ion trapped at the selectivity filter (SF) can be reduced substantially by the pair correlations between ions: the arrival of a second ion at the channel entrance significantly reduces the potential barrier impeding the escape of the ion from the SF. The effects of this rate modulation on the current-voltage and current-concentration characteristics of the channel are studied parametrically. Stochastic amplification of the channel conductivity by charge fluctuations is demonstrated and compared with the results of Brownian dynamics simulations.

PACS numbers: 02.50.Tt, 05.45.Tp, 05.10.Gg, 05.45.Xt
Keywords: ion channels, permeation, nonequilibrium rate, stochastic dynamics, fluctuating barrier

1. Introduction

Ion channels are pathways down the centers of proteins embedded into the membranes of biological cells [1, 2]. Their purpose is to facilitate the diffusion of ions across the cell membranes. To support life, channels have to be precise, often selecting between similar ions with an accuracy of 1:1000 [3], yet still able to deliver millions of ions per second, i.e. almost at the rate of free diffusion. In recent years impressive progress has been achieved both in understanding the structure of ion channels [4] and in modeling their properties [5]. Yet the mechanism that enables channels to be highly selective between alike ions, while still passing millions of ions per second, remains a tantalizing paradox.

Reaction rate theory is one of the oldest and most widely accepted theoretical tools used to account for the operation of ion channels. It can reproduce some important channel properties, including their conductivity and their selectivity be-

*Also at Department of Physics, Lancaster University, Lancaster LA1 4YB, UK
†E-mail: p.v.e.mcclintock@lancaster.ac.uk

tween alike ions. It treats the channels as a set of states, with fixed transition rates between them. The current consensus views the transition rates, and often the states themselves, merely as convenient fitting parameters of the model without having any direct physical meaning. The rationale behind this view is the complexity of real channel dynamics, in which transition rates are modulated by many different factors, including long range interactions with ions in the electrolytes, interactions with fixed charge on the channel wall, the effects of hydration and dehydration of ions within the channel, and wall vibrations. Given this situation, equilibrium reaction rate theory (RRT) with a large number of states and fixed transition rates between them, serves as a first order approximation to the complex non-equilibrium reality.

At the same, the validity of the assumption of constant transition rates, and their lack of physical significance, have often been questioned [6]. It was shown for example that the use of constant rates is inconsistent with experiment [7], and that the modulation of transition rates due to random fluctuations in the electric potential can be used to extract useful work from the energy of non-equilibrium fluctuations [8], e.g. to transport molecules in molecular motors [9].

We seek to account for, and understand, the non-equilibrium stochastic phenomena associated with ionic permeation though an open ion channel. A possible theoretical approach is based on an extension of RRT that takes the abovementioned interactions into account explicitly, using the standard results of stochastic theory. Within this framework it may become possible to reconcile the parameters of the RRT model with the actual properties of the channels and, in particular, with the shape of the channel potentials as obtained from molecular dynamics (MD) simulations. These latter can then be used in Brownian dynamics (BD) simulations.

In this paper we review briefly some recent results derived by this approach and consider its application to the analysis of conductivity in an archetypal open ion channel. We show that the transition rate is modulated by long range pair correlations of the ionic motion, and that this modulation may result in stochastic amplification of the channel conductivity. The predicted stochastic amplification is compared with the results of BD simulations.

The paper is organized as follows. We present in Section 2 a modified archetypal model of the channel. Section 3 develops a simple generalization of RRT that takes into account the ion-ion interactions. Parametric studies of the model are described in Section 4. Predictions based on it are compared with the characteristics of real channels, and with the results of BD simulations, in Section 5, where it is shown that non-equilibrium interactions can amplify the current through the channel. Finally, we summarise the main results, draw conclusions, and outline our perception of future perspectives in Section 6.

2. Model

We will base our simple extension of RRT on a generic model [1, 10, 11] of an ion channel, consisting of a water-filled cylindrical hole through the protein in the cell membrane, with a single binding site around its centre. The channel is open to the bulk solutions on both sides of the membrane, as sketched in Figure 1(a). In standard RRT the channel is modeled as three potential barriers with prescribed transition rates in each direction over their tops, and the rates are treated as fitting parameters in applying the model to any specific kind of channel. To extend this approach by including explicitly the modulation of the rates due to ion-ion interactions, we modify the model in two important respects.

First, we introduce two effective binding sites in the form of hemispheres at each side of the channel as shown in Figure 1(a). The physical significance of these sites is related to the Debye screening of the ionic potential in the electrolyte solutions. Thus, for a typical screening length λ_D of order 5 Å, only ions coming within λ_D of the channel entrance can influence the motion of an ion within the channel. This influence can be quite

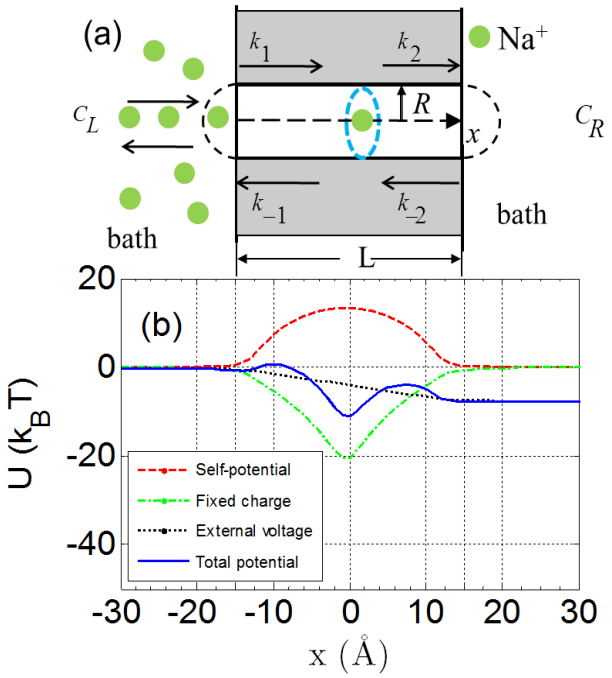

FIG. 1. (Color online) (a) Geometry of the model system under consideration (see text). (b) The total potential energy is made up from a sum of several different contributions. The curves represent (from top to bottom at $x = 0$): the self-potential; the potential due to the externally applied voltage; the total potential energy; and the potential due to the fixed charge. The ends of the channel are at ± 15 Å as indicated by the vertical alignment with the schematic of the model in (a).

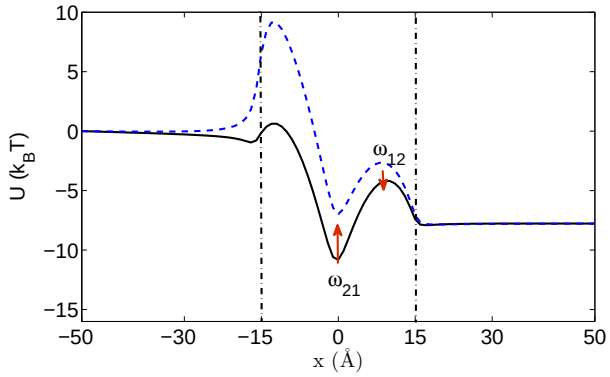

FIG. 2. (Color online) Potential energy along the channel axis, for 200mV applied voltage. The full black line is the potential of a single Na^+ ion moving along the channel axis. The dashed line is the potential acting on a Na^+ ion moving along the channel axis when there is one Na^+ ion at the mouth of the channel. The vertical dash-dotted lines indicate the positions of the ends of the channel. ω_{21} is the average inverse time during which the potential remains deep (full curve) before a Na^+ ion arrives at the left entrance, making the potential shallower (dashed); ω_{12} is the average inverse time during which the potential remains shallow, before the Na^+ ion diffuses away from the channel entrance, thereby returning the potential to its original deep configuration.

significant because the channel acts as an electrostatic amplifier of the ion-ion interaction. The latter phenomenon can readily be understood by consideration of two limiting cases. For very large channel radii the effective dielectric constant ε_{eff} of the channel approaches its value in water, so that the interaction potential $\phi_{corr} \propto 1/\varepsilon_w r$ decays fast. In the opposite limit of small channel radius ($R \to 0$), ε_{eff} approaches its value in the protein, and $\phi_{corr} \propto 1/\varepsilon_p r$ then decays up to 40 times more slowly. In narrow channels the ε_{eff} is expected to be close to the protein value [12], giving rise to a strong amplification of the ion-ion interaction.

Secondly, to characterize the ion-ion interaction we introduce the following physical parameters. The rate at which ions arrive at the left channel mouth is given by the Smoluchowsky rate $1/\tau_{ar} \propto \pi R C_L D$, where C_L is the concentration of ions in the left bath and D is the ionic diffusion constant. The rate at which ions leave the hemisphere is given by the diffusion time $\tau_D \propto R^2/3D$. These estimates were confirmed in our earlier 3D BD simulations [13, 14], where it was shown that the distribution of random arrival times follows an exponential law with the characteristic time given by the inverse of the Smoluchowsky rate. In addition, the parameter characterizing the strength of the interaction is introduced as a change in the depth of the exit potential barrier for an ion trapped at the binding site when the second ion arrives at the channel mouth.

The change in the potential barrier at the channel exit can be estimated by taking into ac-

count the almost linear decay of the potential inside the channel [15]. For example, if the second ion is located at a distance 1 Å from the channel mouth and the local potential extrema at the binding site are separated by 7 Å, the potential barrier height is reduced by $\Delta U_2 \approx 1.5\, k_B T$ and the pair correlations exert a leading order effect on ion motion through the channel. These estimates can be further confirmed by explicit solution of the Poisson equation for the single-ion potential profile in the channel both with, and without, the second ion at the channel mouth.

Solutions of the Poisson equation for a single ion are shown in Figure 1 (bottom). The corresponding potential profile consists of the following components: the self-energy due to the image charges induced in the protein walls, the external potential corresponding to the applied potential difference across the cell membrane (i.e. between the two baths), and the potential of the fixed charge on the protein wall. The resultant total potential is show by the full blue line in Figure 1 (bottom). It exhibits a relatively deep potential minimum at the center of the channel, corresponding to the binding site, and two potential barriers impeding exit to the right and to the left respectively.

With a second ion present at the left channel mouth, there is an additional contribution due to the ion-ion interaction which modifies the single ion potential as shown by the dashed curve in Figure 2. It is evident that the modified potential has a lower barrier impeding exit to the right. The change F_{corr} in the height of the potential barrier, found by solution of the Poisson equation, is of the order of 1.5 $k_B T$ in agreement with the above estimates. For escape processes that occur on the timescale of a few tens of nanoseconds, only the averaged position of the second ion at the channel mouth has physical significance. The corresponding fluctuations of $U(x)$, averaged in time, can be modeled as dichotomous noise.

Note that, without having introduced any fitting parameters into the model, we arrive naturally at a situation where the single-ion potential of the channel is flipping between two states. The flipping rate to the state with decreased potential barrier (state 2) is given by the Smoluchowsky arrival rate $\omega_{21} = J^l_{ar}$, and the rate of return to the single-ion state with the larger potential barrier (ground state 1) is given by the diffusion rate $\omega_{12} = k^l_{ref}$. The two different potential barrier configurations result in two different escape rates of the trapped ion out of the channel. In order to describe this situation we introduce in Section 3 a modified form of RRT that takes into account the non-equilibrium modulation of the escape rate.

3. Non-equilibrium rate theory

The model introduced above has three sites: the binding site at the center of the channel; and an effective site at each of the channel mouths. The rate k_2 at which ions escape to the right from the binding site is a function of the model parameters that characterize the interaction between the ion at the binding site and ions arriving at random at the left channel mouth. We will develop a theory of the stochastic transition of ions through the channel below, in two stages.

First, we neglect the ion-ion interactions and apply standard RRT in Section 3 3.1 to calculate the current J through the channel using constant reaction rates, arriving at the simple formula $J = k_2 P_0$. Secondly, in Section 3 3.2, we include the interactions and calculate the dependence of k_2 on the model parameters ω_{12}, ω_{21}, and ΔU_2. The results of these calculations are investigated parametrically and compared with the results of BD simulations in Section 4.

3.1. Reaction Rate Theory for ion channels conduction

The kinetic equations for the model presented in Sec. 2 are given by RRT (cf. [10]):

$$\begin{aligned} \dot{P}_0 &= k_1 P_l (1-P_0) - (k_{-1}+k_2) P_0 \\ &\quad + k_{-2} P_r (1-P_0), \\ \dot{P}_l &= J^l_{ar} - k^l_{ref} P_l - k_1 P_l (1-P_0) + k_{-1} P_0, \\ \dot{P}_r &= J^r_{ar} - k^r_{dif} P_r + k_2 P_0 - k_{-2} P_r (1-P_0). \end{aligned} \tag{1}$$

Here $J^{l,r}_{ar}$ are the constant arrival rates at which ions are injected respectively into the left and right volumes located at the mouths of the channel. $P_{l,r}$ are respectively the occupation probabilities of the left and right volumes. P_0 is the probability of occupation of the charged binding site in the middle of the channel. $P_{l,r}(1-P_0)$ ensures that an ion can only enter an empty channel from the left or the right mouth. k^l_{ref} and k^r_{dif} are respectively the diffusive reflection rates at the left and right mouths of the channel. The current from the left to the right, or from the right to the left, mouth of the channel is given by:

$$\begin{aligned} J &= k_1 P_l (1-P_0) - k_{-1} P_0 \\ &= k_2 P_0 - k_{-2} P_r (1-P_0). \end{aligned} \tag{2}$$

Looking for the steady state current, we write:

$$\begin{aligned} J^l_{ar} - k^l_{ref} P_l - J &= 0, \\ k_1 P_l (1-P_0) - (k_{-1}+k_2) P_0 & \\ + k_{-2} P_r (1-P_0) &= 0, \\ J^r_{ar} - k^r_{dif} P_r + J &= 0. \end{aligned} \tag{3}$$

The ion injection rate on the left is given by: $J^l_{ar} = 2\pi R C_L D$. When the channel is closed, the occupation probability of the left hemisphere at the channel mouth is given by $P_l = 2\pi R^3 C_L$, where R is the radius of the hemisphere. The ion injection rate and the occupation probability from the right mouth are written similarly. The diffusive reflection rates at the left and right mouths k^l_{ref} and k^r_{dif} are calculated from the stationary solution when the channel is non-conducting ($J = 0$); this leads to

$$k^l_{ref} = \frac{3D}{R^2}, \tag{4}$$

$$k^r_{dif} = \frac{3D}{R^2}. \tag{5}$$

Combining the elements of the steady state equation leads to a second order equation in P_0. The current can then be calculated as:

$$J = \frac{k_1 (1-P_0) J^l_{ar} - k^l_{ref} k_{-1} P_0}{k^l_{ref} + k_1 (1-P_0)}. \tag{6}$$

The occupation probabilities of the left and right mouths of the channel are given respectively by:

$$P_l = \frac{J^l_{ar} - J}{k^l_{ref}}, \tag{7}$$

$$P_r = \frac{J}{k^r_{dif}}. \tag{8}$$

We are interested in the particular case of unidirectional current. The concentration on the right hand side of the channel is therefore set to zero: $C_R = 0$. Since there is no backflow from the right bulk to the left bulk, we set $k_{-2} = 0$. For small values of the k_2 parameter, corresponding to $J \ll J^l_{ar}$, the channel binding site occupancy is given by:

$$P_0 = \frac{k_1 J^l_{ar}}{k_1 J^l_{ar} + (k_2 + k_{-1}) k^l_{ref}}, \tag{9}$$

and the corresponding current is given by:

$$J = k_2 P_0. \tag{10}$$

Note that the current through the channel in this strongly asymmetric situation depends only on the two variables k_2 and P_0. In standard rate theory k_2 is constant and the current is then expected to follow the well-known Michaelis-Menten kinetics [1, 16], exhibiting saturation of P_0 as a function of J^l_{ar}. However, if the interactions between ions cannot be neglected, the escape rate k_2 becomes a function of J^l_{ar} and k^l_{ref}. As a result the current through the channel may deviate markedly

from the Michaelis-Menten form, demonstrating stochastic amplification.

To seek further insight into the influence of the ion-ion interaction on the permeation of the channel, we now introduce in Section 3 3.2 a non-equilibrium extension of RRT by calculation of the dependence of k_2 on the interaction parameters.

3.2. Fluctuating Barrier Theory

To take account of ion-ion interactions, and to calculate the escape rate k_2 as a function of the flipping rates and the corresponding modulation of the potential barrier $k_2 = k_2(\omega_{12}, \omega_{21}, \Delta U_2)$, we notice that the modulation of the potential is strongly non-equilibrium. This is because at least one rate ω_{12} is of the order of the inverse diffusion time, which is close to the relaxation time of the ion to the potential minimum.

Thus, k_2 has to be calculated using Chapman-Kolmogorov theory [17] for mixed diffusion-jump processes. Accordingly, we seek the probability density $P_i(x,t|y,t'=0)$ of the stochastic variable, starting at $t'=0$ at position y, to exit the channel either at x_1 or x_2, while the system displays mixed dynamics, jumping with the rate $\omega(j|i,t')$ between the potential states i and j that have drift and diffusion coefficients $A_{i,j}$ and $B_{i,j}$ respectively:

$$\partial_{t'} P_i(x,t|y,t') = -A_i(y,t')\partial_y P_i(x,t|y,t') - \frac{1}{2}B_i(y,t')\partial_y^2 P_i(x,t|y,t') + \sum_j \omega(j|i,t')[P_j(x,t|y,t') - P_i(x,t|y,t')]. \tag{11}$$

Following Gardiner [17] we seek the probability density $P_i(x,t|y,0)$ for the stochastic variable, starting at $t'=0$ at position y, to exit the channel either at the left or the right barrier top. Using the standard formalism [17] the mean value of the exit time, the so-called mean first passage time (MFPT) $\tau(y)$, can be expressed via $P_i(x,t|y,0)$ as

$$\tau(y) = \int_0^\infty \int_{x_0}^{x_1} P_i(x,t|y,0)dxdt, \tag{12}$$

where x_0 is the potential minimum and x_1 is the potential maximum close to the right mouth.

To estimate the escape rate we analyze the case of the two-state potential both without, and with, one positive ion at the left channel mouth (as shown in Figure 2), setting the ionic concentration in the right bulk solution to zero ($C_R = 0$). In this case the solution of the Eq. (11) can be reduced [18, 19] to the analysis of the following system of equations [20]

$$\begin{aligned} \tau_1' &= S_1 \\ \frac{k_B T}{m\gamma} S_1' &= \frac{1}{m\gamma}\phi_1' S_1 + \omega_{21}(\tau_1 - \tau_2) - 1 \\ \tau_2' &= S_2 \\ \frac{k_B T}{m\gamma} S_2' &= \frac{1}{m\gamma}\phi_2' S_2 + \omega_{12}(\tau_2 - \tau_1) - 1, \end{aligned} \tag{13}$$

supplied with boundary conditions $\tau_i'(x = x_0, t) = 0$; $\tau_i(x = x_1, t) = 0$. The escape rate $k_2 = 1/\tau_1$ can now be found as a solution of the boundary value problem (13).

We are now in a position to investigate non-equilibrium phenomena associated with channel permeation for different sets of parameters.

4. Parametric study of the model

As discussed above, the escape rate k_2 is a function of several parameters and, in particular:

the ions' arrival rate $\omega_{21} = J^l_{ar}$; their diffusion rate $\omega_{12} = k^l_{ref}$; and the strength of their mutual interaction ΔU_2. We now consider the effect of changes in each of these quantities.

4.1. Dependence on the flipping rates

To consider the dependence of the escape rate on the flipping rates we note that the $w_{21} = J^l_{ar} \propto \pi R C_L D$, so that the dependence on w_{21} can be interpreted in terms of concentration C_L in the left bulk solution. On the other hand the flipping-back rate $w_{12} = k^l_{ref}$ does not depend on the concentration (but, rather, corresponds to how long the ion at the left mouth takes to diffuse away). In real channels, however, the potential profile will depend on the precise geometry and on possible additional small fixed charge at the channel mouth. It is therefore of interest to analyze the dependences of the escape rate and current as functions of both w_{21} and w_{12}.

Note that an increasing concentration leads to an increasing w_{21} and more frequent modulation of the unperturbed potential. Since the modified potential barrier is reduced by an increment ΔU_2, it is expected that the more frequent arrival of ions at the channel mouth may result in a significant increase of the escape rate k_2 and thus of the channel current.

On the other hand, an increasing w_{12} means that after arrival the ion will spend less time at the channel mouth, and hence that the potential barrier will spend more time in its unperturbed state. It is therefore expected that the escape rate k_2 and the channel current will both be decreasing functions of the w_{12}.

Calculations of the k_2 as a function of $w_{21} = J^l_{ar} \propto \pi R C_L D$ are presented in Figure 3 for different values of w_{12}. It can be seen that, as expected, the escape rate k_2 is an increasing function of the concentration and a decreasing function of w_{12}.

Another interesting feature evident in the figure is that the $k_2 - C$ curves take the well-known sigmoid shape also known as Hill's curve [21, 22]. For example Hill's curve was found

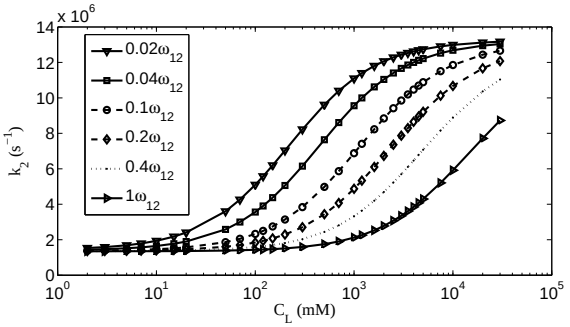

FIG. 3. Escape rate k_2 as a function of the left-bath concentration C_L and reflection diffusion rate ω_{12} (shown in key) of ions at the left mouth. The potential difference applied across the channel was $V_{app} = 200$mV.

in the calcium-activated potassium channel [23], in which an additional binding site exists for Ca ions. Thus our theory offers an alternative derivation of Hill's curve based on the fundamental electrostatic properties of the channel.

To obtain the current we note that, as shown above in Sec. 3, $J = k_2 P_0$, where the channel population P_0 is given by Equation (9), which is a nonlinear function of both $J_{ar} \propto C_L$ and k_2. The channel population and the resulting current calculated within formalism of non-linear RRT are shown in Figure 4.

The main result of this analysis is the prediction of a strong increase of the current through the channel as a function of both ionic concentration and ionic residence time at the channel mouth. Note that there is an important difference between this picture and the standard knock-on mechanism, and between their predictions. Here, the second ion does not, on average, enter the channel at all.

The results of Figure 4 corroborate this picture by showing that the current increase corresponds to the plateau region where the channel population remains at saturation level, with a single ion occupying the channel nearly all the time. This fact is very important from the point of view of applications. Consider for example a situ-

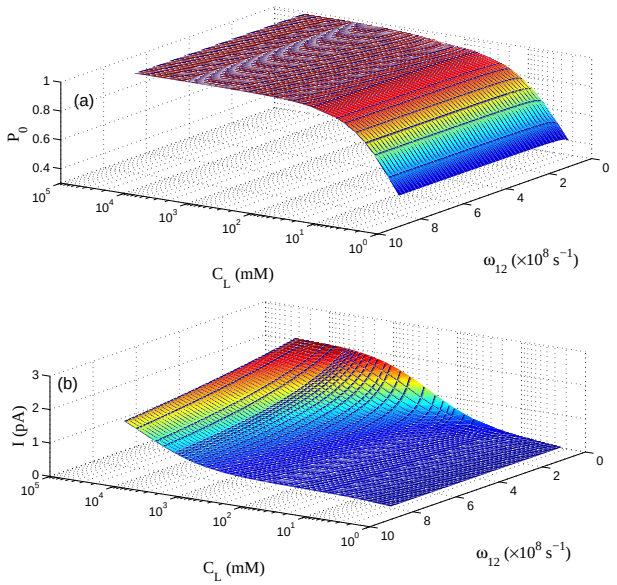

FIG. 4. (Color online) (a) The channel population as a function of the left-bath concentration C_L and the average inverse diffusion time w_{12} of the second Na^+ ion away from the channel entrance. Here, $\Delta U_2 \approx 1 k_B T$ and the potential difference applied across the channel was $V_{app} = 200$mV. (b) The corresponding permeating current.

ation when the conducting ions are mixed with another type of ion in the solution in the ratio 1:20. The mechanism proposed above suggests that the more-abundant ions will arrive at the channel mouth at a rate 20 larger than that of the conducting ions. Upon arrival they will strongly modulate the single-ion potential for the conducting ion occupying the channel, thereby facilitating completion of the permeation process.

We conjecture that the proposed mechanism can he used to extract useful work from the non-equilibrium modulation of the fluctuating channel potential due to the frequent arrival of the more-abundant non-conducting ions. For example this energy can switch the channel between different conformational or dynamical states.

4.2. Dependence on the strength of the interaction

We now turn to an analysis of stochastic amplification of the channel current, as a function of the interaction strength. As discussed in Sec. 2, the strength of the ion-ion interaction in this system can be characterized by the change ΔU_2 in the potential barrier height for ions exiting to the right from the binding site.

Within our electrostatic model of channel conductance, the strength of the potential modulation is characterized by: (i) the locations of the potential extrema; (ii) the distance between the potential minimum and the right-hand maximum; and (iii) the effective averaged position of the second ion at the left channel entrance. The first two factors are determined mainly by the distribution of fixed charge on the channel wall. In the present case we consider the latter distribution to be constant, and our analysis is therefore restricted to the dependence of the exit rate on the effective location of the second ion near the channel mouth.

In real channels the location of the second ion can be affected by various factors including the precise geometry and the possible presence of weak additional charge at the channel mouth. The effective location of the second ion at the channel mouth can also be a function of the concentration. Indeed, when the concentration increases the Debye screening length decreases as $\propto 1/\sqrt{C_L}$.

Even small variations in the effective location of the second ion may result in marked changes in the strength of the interaction. This is because the ion's potential decays as $\propto 1/d$, where d is the distance between the ion and the channel entrance plane. Because of this singular behavior we expect that even small (of order 0.5Å) changes in the effective ion location will result in significant changes in the modulation of the potential due to the ion-ion interaction. Furthermore, even small changes in the amplitude of modulation will lead to substantial changes in the current through the channel.

To illustrate this point we consider the de-

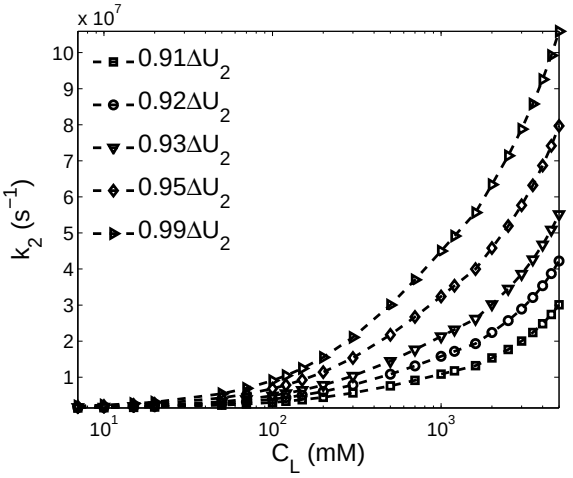

FIG. 5. Escape rate as a function of concentration for different values of channel's exit barrier height, ranging from $0.91\Delta U_2$ and $0.99\Delta U_2$, as indicated in the key. The potential difference applied across the channel was $V_{app} = 200$mV.

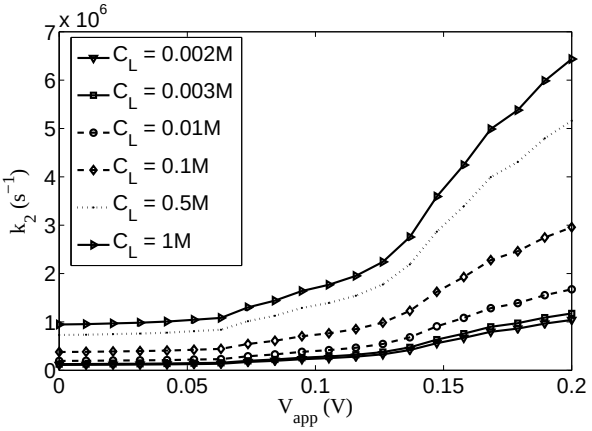

FIG. 6. The escape rate k_2 as a function of the potential difference V_{app} applied across the channel, for the left-bath concentrations shown in the key.

pendence of the escape rate k_2 on the amplitude of the channels' exit barrier modulation ΔU_2, for various concentrations of ions in the left bulk solution. We restrict the changes in the potential modulation to small values of a few % between $0.91\Delta U_2$ and $0.99\Delta U_2$. The results of the corresponding calculations are plotted in Figure 5.

It can be seen from the figure that, in agreement with the above considerations, above even a very small (less than 1%) increase in the modulation depth of the ΔU_2 results in a more than four-fold increase of the exit rate and thus of the channel current.

To conclude our discussion of parametric studies, we now consider the current-voltage characteristics of the model for different concentrations of ions in the left bulk.

4.3. Current as a function of the applied voltage and concentration

In considering the current-voltage characteristics, we recall that the contribution of the externally applied voltage to the total channel potential (see Figure 1) is a linearly-decaying function. As a result the potential barrier at the channel exit decreases linearly with applied voltage. For example the height of the potential barrier is decreased by $\approx 2k_BT$ when an external voltage $V_{app} = 200mV$ is applied across the channel.

If the ion-ion interaction is not taken into account, the exit rate for an ion starting from the bottom of the potential x_a to reach the top of the potential barrier x_b can be estimated using Kramer's formula

$$r_K = \frac{D\sqrt{U''(x_a)|U''(x_b)|}}{2\pi k_B T} \times \exp\left(-\frac{(U(x_a) - U(x_b))}{k_B T}\right). \qquad (14)$$

It is thus expected to be an exponential function of applied voltage, and not to depend on the concentration. In this case, according to Eq. (10), the current across the channel will depend on the concentration only via the channel population P_0. This latter dependence is a saturating function of concentration of the Michaelis-Menten type.

When the ion-ion interaction is present it will reveal itself in two respects. First, the escape rate will become an increasing function of the concentration due to the increasing rate of modulation of the escape potential. Secondly, the relative

depth of the potential barrier modulation will increase with the applied voltage, because the absolute value of the barrier will decrease, whereas the change of the potential due to the ion-ion interaction does not depend on the applied voltage. In other words, we expect a super-exponential dependence of the escape rate k_2 on the value of the applied voltage.

Both of these characteristic features of the ion-ion interaction can be seen in the calculated dependence of the escape rate on the applied voltage, for different values of the concentration, as shown in the Figure 6. The dependence of the escape rate on the concentration can be seen in the figure as an overall upwards shift in the $k_2(V_{app})$ curves as the concentration is increased.

Finally, we note that in the absence of ion-ion interaction the channel current was expected to be independent of the concentration in the region of saturated channel population, while non-equilibrium RRT predicts strong increase of the current in this region. The results of these latter predictions are shown in Figure 7. The strong increase of the current in the region where population P_0 is saturated is clearly evident.

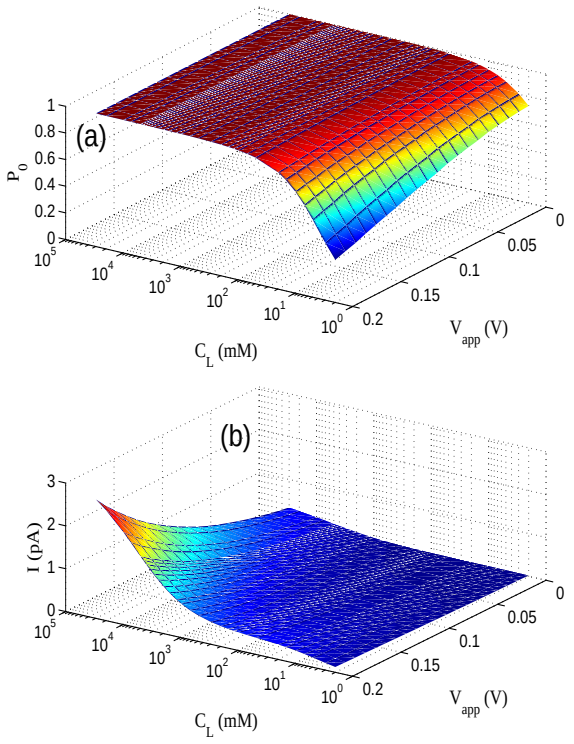

FIG. 7. (Color online) The permeating current as a function of the left-bath concentration C_L and the potential difference V_{app} applied across the channel.

To verify the predicted features of the ion channel current in the presence of the ion-ion interaction we performed BD simulations, as described below.

5. Comparison with BD simulations

5.1. Model Equations

The BD simulations of the model described in Sec. 2 and shown in the Figure 2 are based on the integration of the Langevin equations (15) for interacting ions moving along the channel axis, coupled to simultaneous solution of the Poisson equation (16) for the channel, considering both fixed and mobile charges in an axisymmetric geometry.

The motion of interacting ions of mass m and charge q through the channel is modeled using the overdamped coupled Langevin equations

$$m\gamma\frac{dx_i}{dt} = q\mathcal{E}_i + F_{i,corr} + \sqrt{2m\gamma k_B T}\xi_i(t). \quad (15)$$

The terms on the left-hand side represent Coulomb, frictional, and random forces respectively. The latter is a zero-mean, Gaussian, random force due to the fluctuating environment. It is related to the frictional force via the fluctuation-dissipation theorem [24, 25]. $\mathcal{E}$ denotes the electric field at the ion's position due to the fixed charge of the protein, the membrane potential, and the surface charge induced at the protein-water interface.

The term F_{corr} corresponds to the interaction of the ion at the binding site with other mobile ions. This term is always present in BD simulations (see e.g. [25]). However, in the transition from BD simulations to further theoretical

approximations, such as RRT [10] or the Poisson–Nernst–Plank (PNP) equation [24, 26], the effect of this interaction on the escape rate from the binding site is usually neglected.

The Poisson equation is given by:

$$\nabla \cdot [\varepsilon(\mathbf{r})\nabla\tilde{\phi}(\mathbf{r})] = -\left[\sum_{i=1}^{N} q_j \tilde{n}_j(\mathbf{r}) + \tilde{p}_{fx}(\mathbf{r})\right] \quad (16)$$

where q_j is the charge of the j-th ion and p_{fx} is the fixed charge distribution on the channel wall. The channel is modeled as a cylindrical tube of length L and radius R with a fixed charged ring at its middle, as illustrated in Figure 1.

5.2. Coupled solution of Langevin and Poisson equation using a lookup table

To solve Equation (16) we use a finite-volume method discretized on a staggered rectangular grid. The solver is able to accommodate the severe jumps in dielectric permittivity typical of ion channels ($\varepsilon_w = 80$ and $\varepsilon_p = 2$ respectively for water and protein) and allows one to calculate the electrostatic potentials (see Figure 2) and forces in ion channels, including the image forces acting on ions near the water-protein boundary, the self-potential arising from the membrane protein, the contribution to the potential due to the fixed charge located at the channels' binding site, and the contribution of the external voltage applied across the channel.

The BD simulation involves solving Poisson equation for each time step of ions in Langevin equation. This process is very time-consuming especially in the bulk where ions spend most of the time during the simulation. To facilitate the numerical integration, the potential energy for a single ion was stored in a table for all locations of the ion along the channel axis. To calculate the field for an arbitrary number of ions in the system, the principle of superposition was used.

5.3. Charge fluctuations and injection

Since our primary target is to calculate ion conduction due to ions crossing the channel a further reduction of the simulation time is possible by avoiding the time-consuming simulation of the bulk solution. We have shown numerically in our earlier work that such a reduction is possible because ionic arrivals at the channel mouth from the bulk solution is governed by the Smoluchowski arrival rate [14] at the channel mouth. For this reason, simulations in the bulk solution could be neglected by, instead, injecting ions using the Smoluchowski arrival rate near the channel entrance and allowed them to diffuse on the axis. During this process, the majority of the ions in the simulations diffused away from the channel; occasionally a single ion entered the channel and continue to fluctuate near the SF binding site. Eventually this ion exited the channel by hopping over the exit potential barrier. The corresponding ion current was calculated by counting the number of ions passing the channel per unit of time. Further details of the simulation and the validation of the algorithm can be found in e.g. [14].

5.4. Comparison with gA channel

Before illustrating the phenomenon of stochastic amplification in the BD simulations, we first demonstrate that our proposed non-equilibrium version of RRT is indeed an extension of standard RRT, and can reproduce its results for corresponding values of the model parameters. ln doing so we also wish to demonstrate that non-equilibrium RRT is capable of reproducing the experimentally measured current-concentration ($I - C$) characteristics of real ion channels. To this end we compare the model predictions with the experimentally measured $I - C$ characteristic of the gA channel [20].

The results of the comparison are shown in Figure8. It can be seen that, for the parameters of this channel, the theory is in reasonable agreement with the experimental data, as well

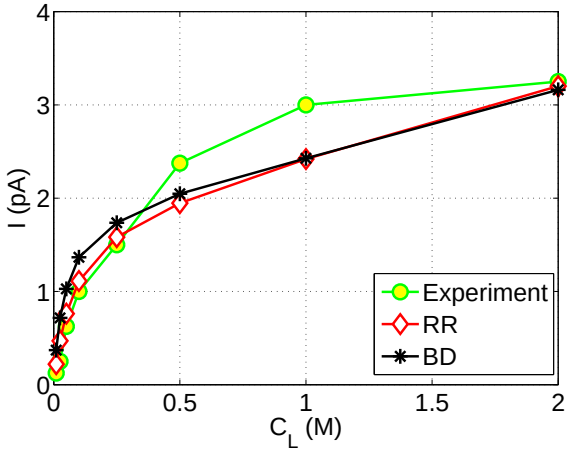

FIG. 8. (Color online) Permeating current I of Na^+ ions in the gA channel, as a function of left-bath concentration C_L, with a potential difference of 200mV applied across the channel. Experimental data from Andersen *et al.* [27] are plotted as circles. The lozenges represent calculations based on the modified rate model; and the stars are from the BD simulations.

as with the BD simulations, and that it demonstrates standard Michaelis-Menten kinetics.

We now apply BD simulations to verify the possibility of stochastic amplification predicted in the current research.

5.5. Stochastic amplification of the channel current

We have performed BD simulations of the current through the open ion channel for the selected model parameters: length $L = 30$Å; radius $R = 4$Å; and fixed charge at the binding site $-0.81e$. BD simulations of the current-concentration dependence for an applied voltage of 200 mV are shown by the blue circles in Figure 9. These results dependence exhibit saturation, with standard near Michaelis-Menten kinetics, up to a concentration $C_L \approx 200$ mM. For higher concentrations a strong stochastic amplification of the channel current can be observed. The BD simulation results are compared with those from non-equilibrium RRT (see Sec. 4 4.3) as shown by the grey surface. The deviations of the current from Michaelis-Menten kinetics above 200 mM were predicted by the parametric studies discussed in Sec. 4 4.1 and illustrated in the Figure 3.

However, an unexpected *additional* stochastic amplification of the channel current was observed in the BD simulations. It can be seen in the figure as a deviation of the BD results (blue circles) from the red line corresponding to the predictions of non-equilibrium RRT. We attribute this additional amplification to the shift with increasing bulk concentration in the effective (averaged) position of the 2nd ion at the channel mouth. This effect can readily be understood on the basis of the parametric studies in Sec. 4 4.2, where it was shown that a small shift in the ion's location near the channel mouth results in a small change in depth of the potential modulation ΔU_2, leading in turn to a marked increase in current.

We are able to observe the corresponding small shift in the averaged ion location in the BD simulations. This shift is clearly seen e.g. in the conditional PDF shown in the Figure 10 (see below).

The prediction of our modified RRT, taking account of small shift in the location of the second ion at the left channel, is shown by the dashed blue line in Figure 9: the agreement is clearly very good, and we conclude that theory is then able to describe accurately all the characteristic features of the current-concentration dependence that appear in the BD simulations.

We now discuss in detail how the proposed mechanism of stochastic current amplification differs from the well-known knock-on mechanism of channel conductance, and illustrate how this difference can clearly be detected in the BD simulations.

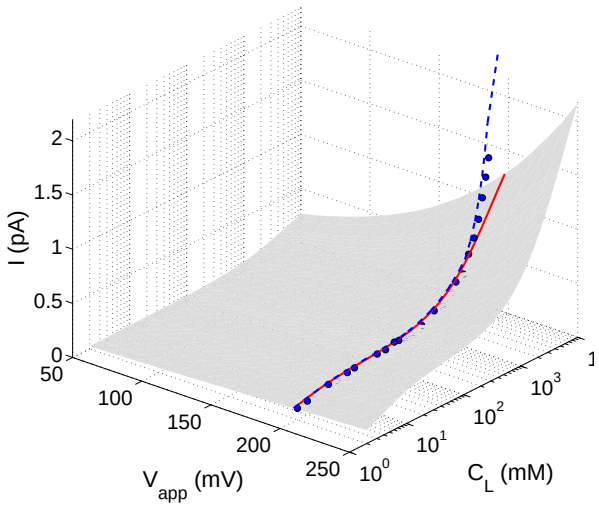

FIG. 9. (Color online) The permeating current I as a function of the left-bath concentration C_L and applied voltage V_{app}, calculated by modified RRT (the grey surface). The results of BD simulations (blue circles) are shown with $V_{app} = 200$mV for comparison; the red line is a smooth curve drawn through their projection onto the surface, as a guide to the eye.

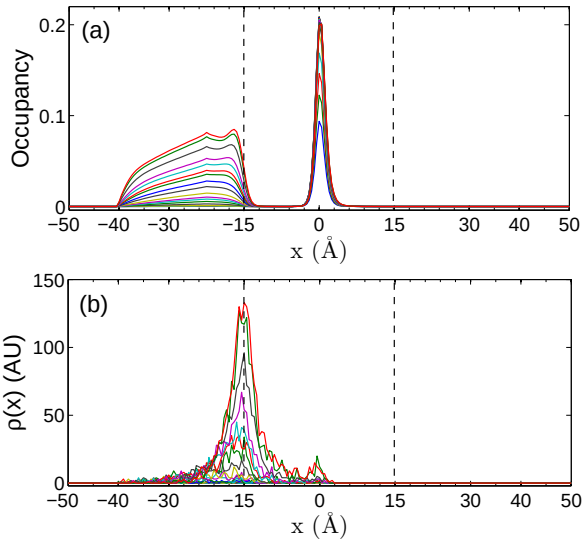

FIG. 10. (Color online) (a) The occupancy as a function of position x, for different values of the left-bath concentration C_L, ranging from 0.002 M (bottom curve) to 4.5 M (top). (b) The conditional probability distribution for the position of the second ion at the moment when the first ion escapes over the exit barrier (see Figure 2, for the same set of concentrations. The vertical dashed lines indicate the positions of the ends of the channel.

5.6. Conditional escape PDF and comparison with standard knock-on model

An equilibrium distribution function $\rho_{st}(x)$ is usually employed to characterize the ion's location in the system. It gives the time-averaged probability of finding an ion at a given location in the system. The corresponding distribution for our model is shown in Figure 10(a) for different concentrations. It is evident that the ion within the channel is sharply localized near the binding site at $x = 0$, while the ionic distribution outside the channel is broad and nearly uniform. It can also be seen from the figure that the channel occupancy, i.e. the averaged probability of finding an ion at any location within the channel, increases with concentration until it reaches its saturation value ≈ 1. Note also that at any concentration the total number of ions outside the channel in our simulations is $\lesssim 1$.

However, the time-averaged distribution of ions within the system does not allow one to characterize the strength of the ion-ion interaction or its effect on the escape of ions from the binding site.

To measure ion-ion pair correlations in the BD simulations we have introduced a new quantity – the conditional probability distribution $\rho(x) = P(x_2 = x | x_1 \geqslant x_{ex})$ that gives the probability of finding a 2nd ion in the system at location x at the time instant t when the 1st ion is exiting the system, i.e. is located near the top of the exit potential barrier x_{ex}. The conditional PDF $\rho(x)$ is normalized by the total probability of finding ions anywhere in the system.

The conditional probability introduced above allows us to determine the location of the second ion during the escape and thus to discriminate between different escape mechanisms. ln particular, we can distinguish clearly between the standard knock-on mechanism (see e.g [28, 29])

and the mechanism for enhancement of the channel current proposed here. The standard knock-on mechanism, proposed by Hodgkin and Keynes [30], assumes that the second ion enters the channel, lowering the exit potential barrier for the first ion; the first ion then leaves the system, while the second remains in the channel. Effectively, therefore, the second ion pushes the first one out and takes its place at the SF. Some features specific for the standard knock-on mechanism are that: (i) it involves a step when both ions are in the channel; (ii) the second ion remains in the channel when the first leaves it; and (iii) for selective conduction both ions must be of the same type.

In contrast, the mechanism proposed here does not require the second ion to enter the channel; neither does it require both ions to be of the same type. In terms of conditional escape probabilities the two mechanisms can be clearly distinguished as follows. Because the traditional knock-on mechanism requires that the second ion enter the channel and remain there during the escape by the first ion, the conditional PDF $\rho(x)$ should display a peak at the channel binding site, indicating that the 2nd ion is located at the binding site when the 1st ion is exiting the channel. In our proposed mechanism, the 2nd ion can stay outside the channel during the whole escape process. Accordingly, the conditional PDF $\rho(x)$ should display a peak at the channel entrance, indicating that the 2nd ion is as likely to be located outside of the channel as inside it at the moment when the 1st ion is crossing the exit barrier.

Figure 10(b) exhibits a clearly resolved peak in the conditional PDF $\rho(x)$ at the channel entrance. It appears at $C_L \approx 0.5$M and is increasing as a function of concentration, indicating that exit over the potential barrier is strongly correlated with the presence of the 2nd ion at the channel mouth.

Interestingly, a transition to the standard knock-on mechanism is also clearly captured by measurements of the $\rho(x)$. It can be seen from the figure that a second peak in the conditional escape PDF is appearing at the binding site ($x = 0$) for concentrations above $3M$. It clearly indicates that the standard knock-on mechanism is also possible, with the second ion to entering and remaining in the channel during the escape event.

6. Discussion and conclusion

In this review we analyze the influence of ion-ion interaction on the rates at which ions permeate open ion channels. Of special interest to us is the situation that arises when one ion is bound at the selectivity site while the second ion is freely diffusing outside the channel. This situation is quite general, and we have shown that it leads naturally to a strong modulation of the transition rates. To take this modulation into account we introduced a non-equilibrium extension of reaction rate theory, and we performed parametric studies of the channel characteristics on this basis.

We found that the rate at which an ion exits the channel can be strongly enhanced by the concentration, applied voltage, ion location at the channel mouth, and diffusion time of the (external) ion away from the channel mouth. We observed a corresponding enhancement of the channel current as a function of concentration in our Brownian Dynamics simulations, and was showed that it was in good agreement with the theory.

In addition, we found from the BD simulations that the mechanism by which the channel current and be stochastic amplified is distinctly different from the well-known knock-on mechanism, except at the highest concentrations. To distinguish clearly between the two mechanisms we introduced a novel conditional escape PDF. We were thus able to establish that both mechanisms are possible, that they correspond to two different peaks in the conditional PDF, and that a transition occurs between the two mechanisms when the concentration becomes high enough.

The distinguishing feature of stochastic amplification is that, unlike conventional knock-on, the second ion does not on average enter the chan-

nel, which means that it can be of a different type from the conducting ions.

This distinction carries interesting implications for the selectivity *vs.* conductivity paradox, partially resolving it. The paradox can briefly be formulated as follows: strong selectivity requires deep potential wells; but deep potential wells imply low conductivity. The proposed mechanisms resolves this contradiction in the following way. Because the ion arriving from the bath does not need to enter the channel in order to reduce very significantly the escape time of the ion at the selectivity filter, conduction can be enhanced by the presence of different species of ions. So if there are e.g. two types of cations, Na^+ and K^+ in the ratio 20:1, the very presence of the Na^+ ion will enhance the conductivity of the K^+ ions without the Na^+ ion needing to enter the channel.

In conclusion, we have studied the dynamics of ions permeating an archetypal model ion channel. We showed that a modulation of the transition rates arises naturally in ion channels due to long range pair-correlations of the ions. The resultant strong current enhancement occurs prior to the possibility of conventional knock-on taking place place, i.e. the second ion does not have to enter the channel before the exit of the first occurs, so that it is likely to be more widespread and universal.

Acknowledgements

The research was supported by the Engineering and Physical Sciences Research Council UK (grant No. EP/G070660/1).

References

[1] B. Hille, *Ionic Channel Of Excitable Membranes*, Sinauer Associates, Sunderland, MA, 3rd edn. (2001).

[2] R. S. Eisenberg, Ions in fluctuating channels: transistors alive, Fluct. Noise Lett. **11**(1), 1240001 (2012).

[3] D. A. Doyle, J. M. Cabral, R. A. Pfuetzner, A. Kuo, J. M. Gulbis, S. L. Cohen, B. T. Chait, and R. MacKinnon, The structure of the potassium channel: Molecular basis of K^+ conduction and selectivity, Science **280**(5360), 69–77 (1998).

[4] J. D. Stockand and M. S. Shapiro, *Ion channels: Methods and Protocols*, Humana Press, Totowa, N.J. (2006).

[5] S.-H. Chung, V. Krishnamurthy, and O. S. Andersen, *Biological Membrane Ion Channels Dynamics, Structure, and Applications*, Springer (2007).

[6] S. W. Jones, Are rate constants constant?, J. Physiol. **571**(3), 502 (2006).

[7] L. S. Liebovitch and P. Krekora, The physical basis of ion channel kinetics: The importance of dynamics, in H. E. Layton and A. M. Weinstein, eds., *Membrane Transport and Renal Physiology*, vol. 129 of *IMA Annual Workshop on Membrane Transport and Renal Physiology*, pp. 27–52, Springer, New York (2002).

[8] Y. D. Chen, Asymmetry and external noise-induced free energy transduction, Proc. Natl. Acad. Sci. USA **84**, 729–733 (1987).

[9] R. D. Astumian, P. B. Chock, T. Y. Tsong, Y. D. Chen, and W. H. V., Can free energy be transduced from electric noise?, Proc. Natl. Acad. Sci. USA **84**, 434–438 (1987).

[10] D. J. Aidley and P. R. Stanfield, *Ion Channels: Molecules in Action*, Cambridge Univ. Press, Cambridge (2000).

[11] Y. Levin, Electrostatics of ions inside the nanopores and trans-membrane channels, Europhys. Lett. **76**(1), 163–169 (2006).

[12] V. Barcilon, Ion flow through narrow membrane channels: Part I, SIAM J. Appl. Math. **52**(5), 1391–1404 (1992).

[13] D. G. Luchinsky, R. Tindjong, I. Kaufman, P. V. E. McClintock, and R. S. Eisenberg, Ion channels as electrostatic amplifiers of charge fluctuations, in Green, N., ed., *Electrostatics 2007*, vol. 142 of *J. Phys. Conf. Series* (2009).

[14] D. G. Luchinsky, R. Tindjong, I. Kaufman, P. V. E. McClintock, and R. S. Eisenberg, Charge

fluctuations and their effect on conduction in biological ion channels, J. Stat. Mech. **P01010** (2009).

[15] S. T. Cui, Electrostatic potential in cylindrical dielectric media using the image charge method, Mol. Phys. **104**(19), 2993–3001 (2006).

[16] L. Menten and M. Michaelis, Die kinetik der invertinwirkung, Biochem. Z. **49**, 333–369 (1913).

[17] C. W. Gardiner, *Handbook of Stochastic Methods: for Physics, Chemistry and the Natural Sciences*, Springer, Berlin (2002).

[18] U. Zürcher and C. R. Doering, Thermally activated escape over fluctuating barriers, Phys. Rev. E **47**, 3862–3869 (1993).

[19] M. Bier and R. D. Astumian, Matching a diffusive and a kinetic approach for escape over a fluctuating barrier, Phys. Rev. Lett. **71**, 1649–1652 (1993).

[20] R. Tindjong, I. Kaufman, P. V. E. McClintock, D. G. Luchinsky, and R. S. Eisenberg, Nonequilibrium rate theory for conduction in open ion channels, Fluct. Noise Lett. **11**(1), 1240016 (2012).

[21] A. V. Hill, The possible effects of aggregation of the molecules of haemoglobin on its dissociation curve, J. Physiol **40**, iv–vii (1910).

[22] S. Goutelle, M. Maurin, F. Rougier, X. Barbaut, L. Bourguignon, M. Ducher, and P. Maire, The hill equation: a review of its capabilities in pharmacological modelling, Fund. Clin. Pharmacol. **22**(6), 633–648 (2008).

[23] T. M. Ishii, C. Silvia, B. Hirschberg, C. T. Bond, J. P. Adelman, and J. Maylie, A human intermediate conductance calcium-activated potassium channel, Proc. Natl. Acad. Sci. USA **94**(21), 11651–11656 (1997).

[24] R. S. Eisenberg, M. M. Klosek, and Z. Schuss, Diffusion as a chemical reaction: Stochastic trajectories between fixed concentrations, J. Chem. Phys. **102**(4), 1767–1780 (1995).

[25] S. C. Li, M. Hoyles, S. Kuyucak, and S. Chung, Brownian dynamics study of ion transport in the vestibule of membrane channels, Biophys. J. **74**(1), 37–47 (1998).

[26] D. G. Luchinsky, R. Tindjong, I. Kaufman, P. V. E. McClintock, and R. S. Eisenberg, Self-consistent analytic solution for the current and the access resistance in open ion channels, Phys. Rev. E **80**(2), 021925 (2009).

[27] O. S. Andersen, R. E. Koeppe, and B. Roux, Gramicidin channels, IEEE Trans. Nanosci. **4**(1), 10–20 (2005).

[28] P. H. Nelson, A permeation theory for single-file ion channels: One- and two-step models, J. Chem. Phys. **134**, 165102–165114 (2011).

[29] S. O. Yesylevskyy and V. N. Kharkyanen, Barrier-less knock-on conduction in ion channels: peculiarity or general mechanism?, Chem. Phys. **312**, 127–133 (2005).

[30] A. L. Hodgkin and R. D. Keynes, The potassium permeability of a giant nerve fibre, J. Physiol. **128**(1), 61–88 (1955).